Radar Interferometry Example

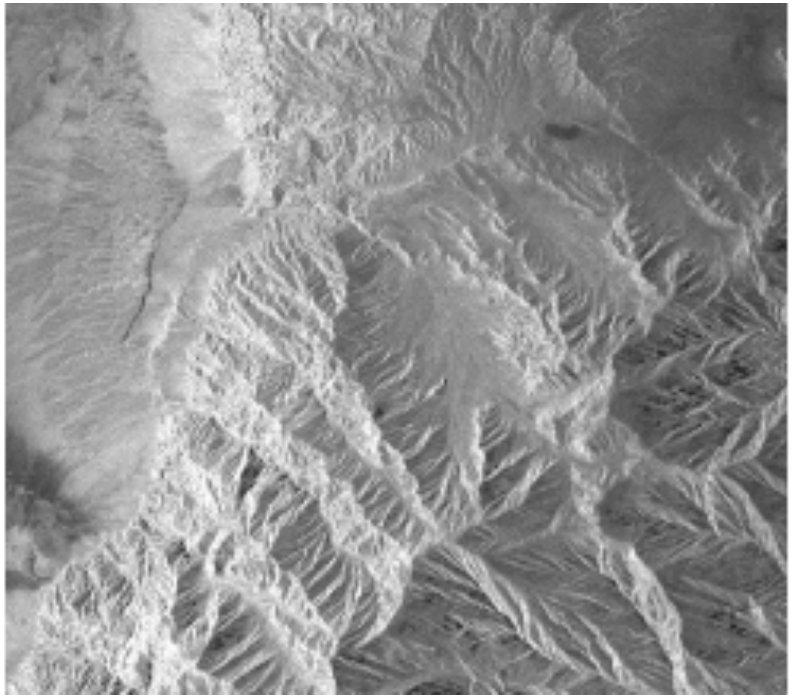

Radar Amplitude Image

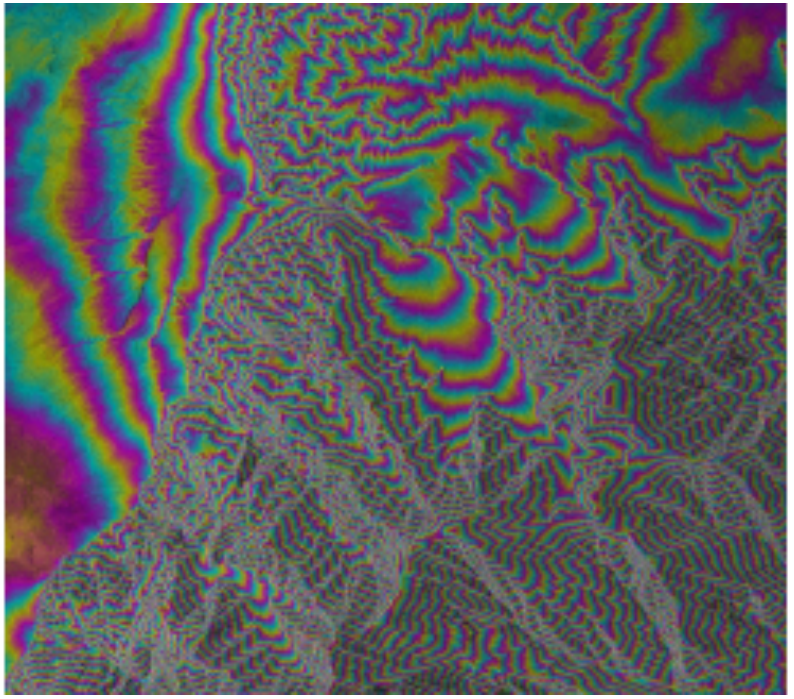

Radar Phase Image

What is Radar Phase?

Phase - A Measure of the Range and Surface Complexity

The phase of the radar signal is the number of *cycles of oscillation* that the wave executes between the radar and the surface and back again.

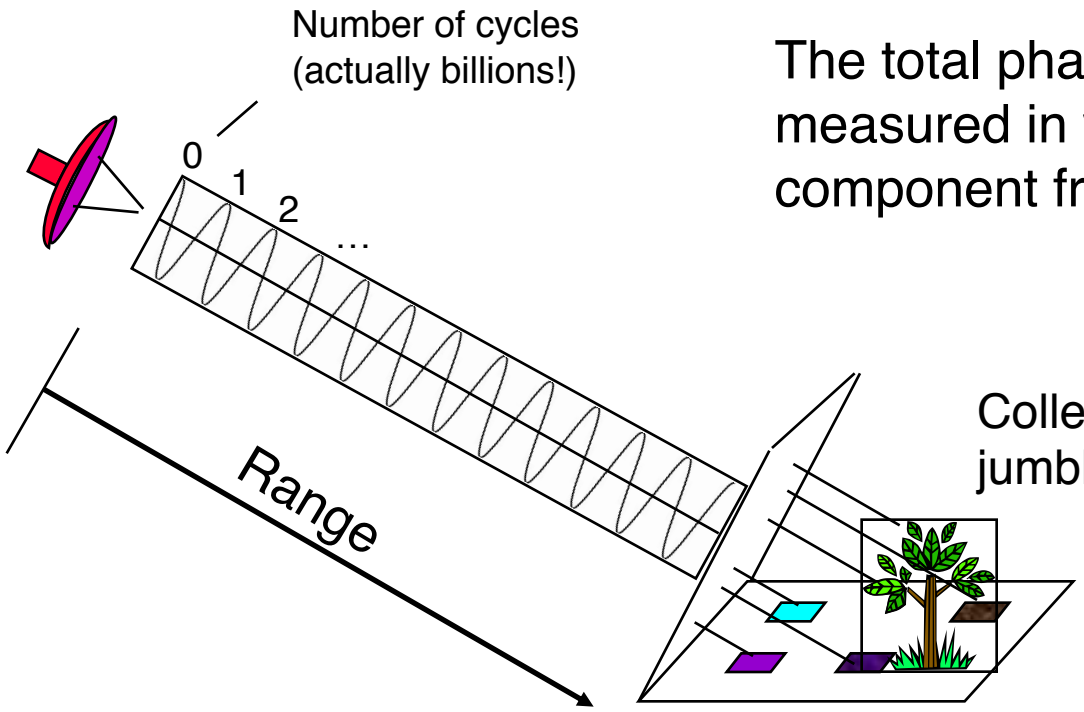

The total phase is two-way range measured in wave cycles + random component from the surface

Collection of random path lengths jumbles the phase of the echo

Only *interferometry* can sort it out!

Image A - 12 August 1999

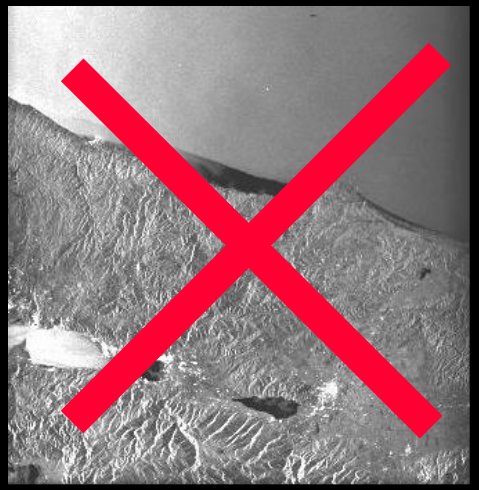

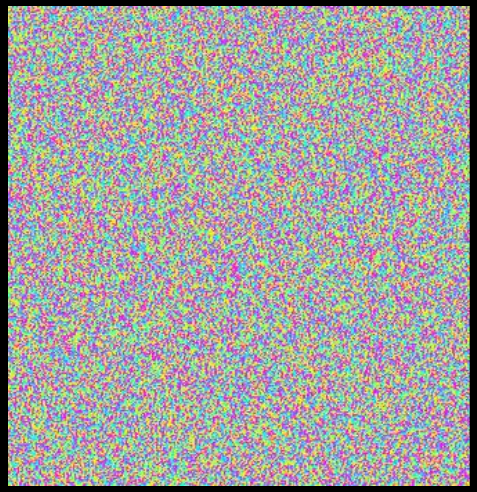

SAR image

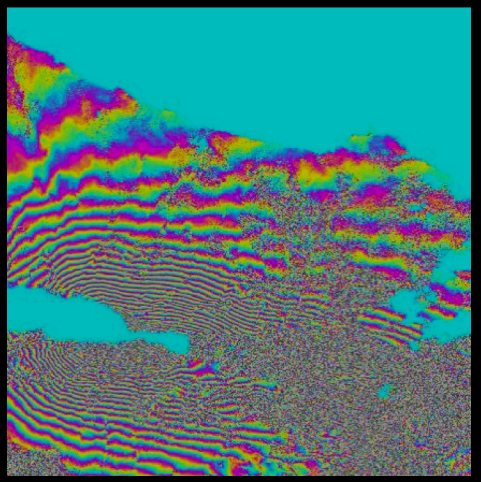

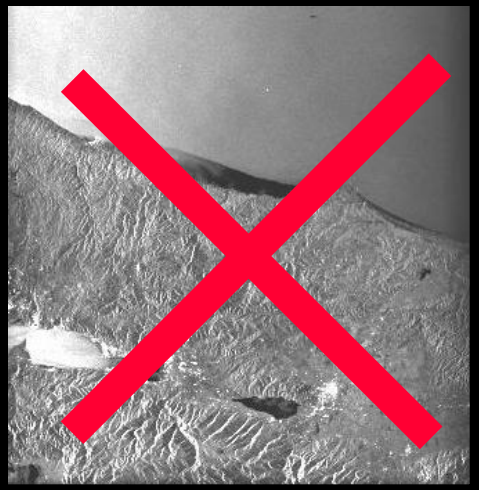

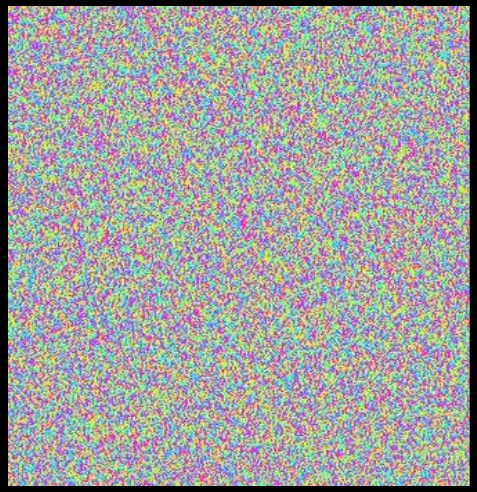

Image B - 16 September 1999

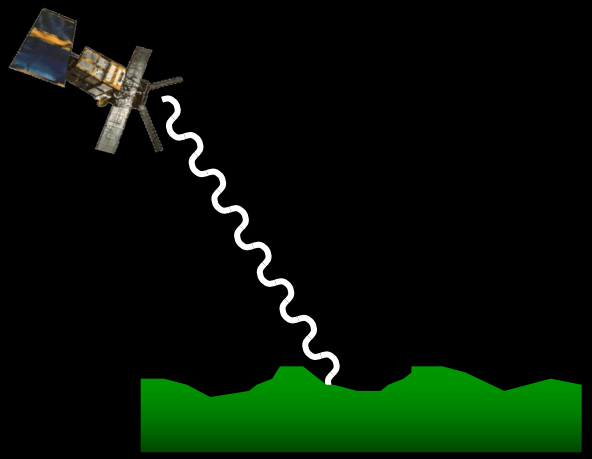

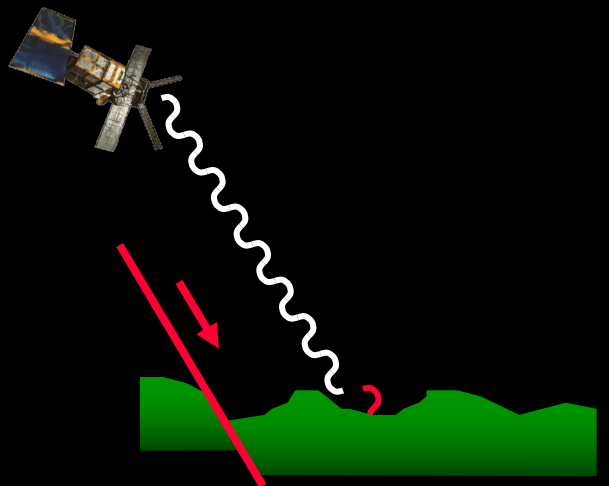

Interference Concept

- Interference occurs when the phase of two different waves is not aligned. The observed intensity, I, is the time average of the sum of the wave fields

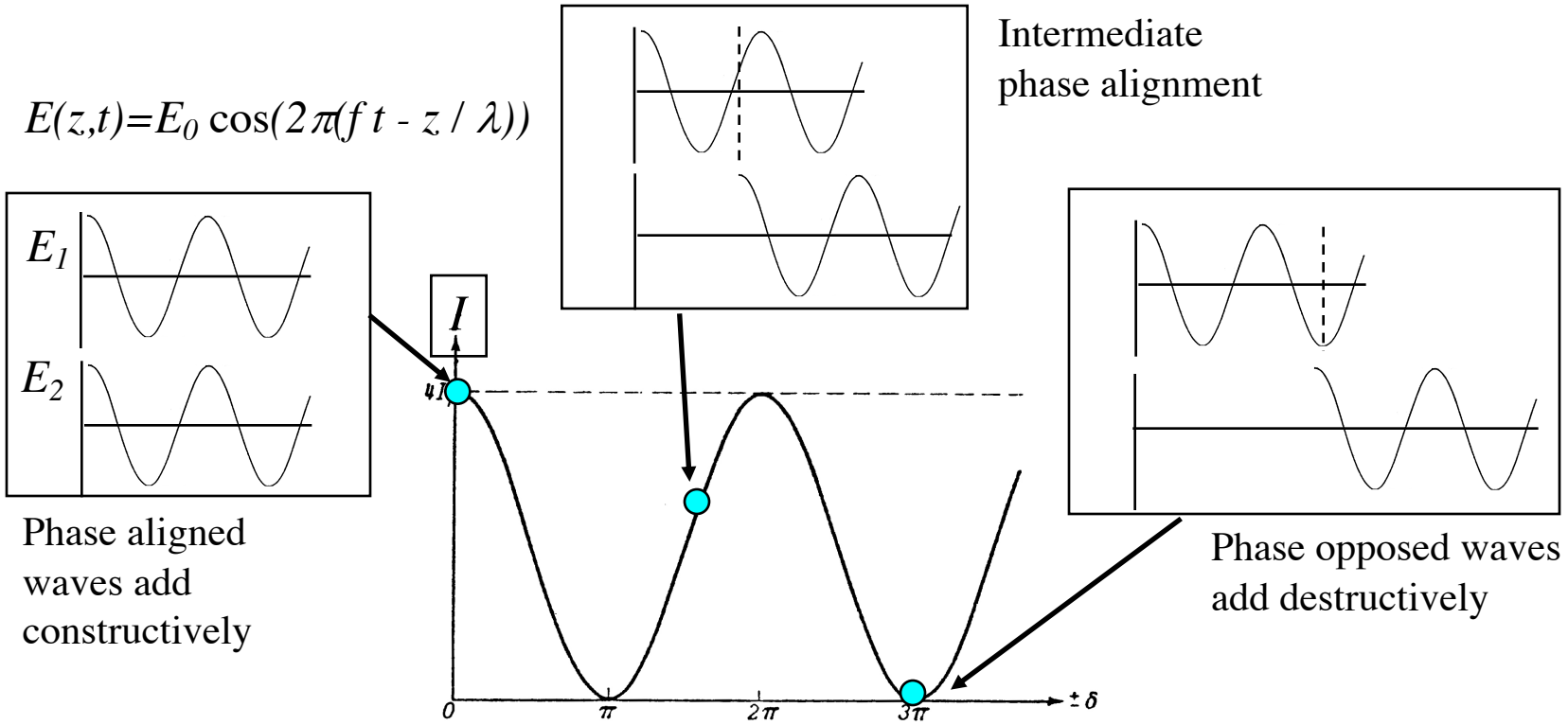

Fig. 7.1. Interference of two beams of equal intensity; variation of intensity with phase difference.

Young's Interferometer

- In Young's experiment, a point source illuminates two separated vertical slits in an opaque screen. The slits are very narrow and act as line sources. For this case, the pattern of intensity variations on the observing screen is bright/dark banding.

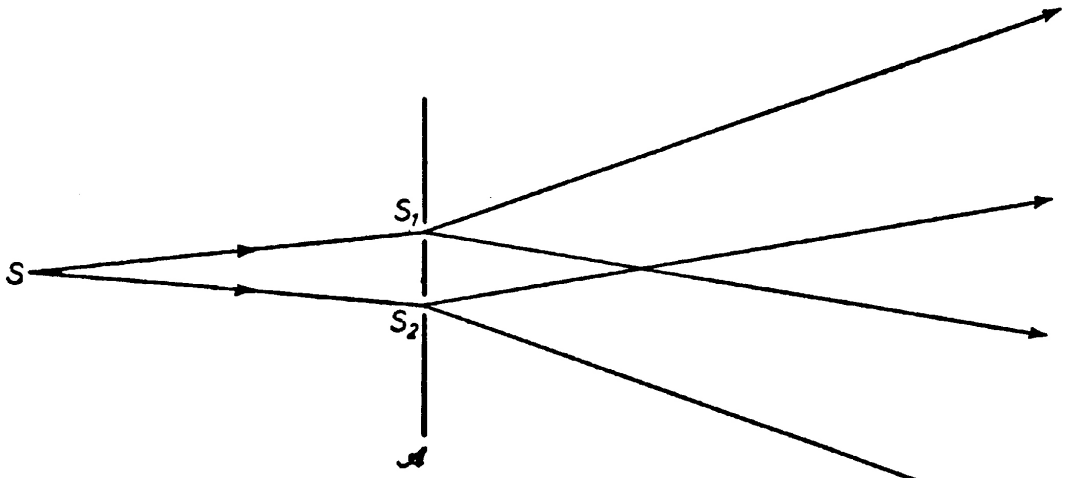

Fig. 7.2. YOUNG's experiment
(Born and Wolf, 1980)

Observing Screen

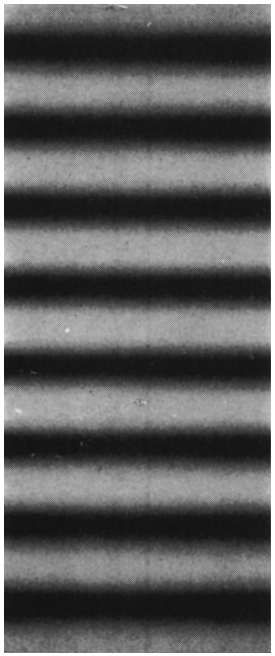

Screen laid flat

Young's Interferometer Geometry

- The brightness variations can be understood in terms of the relative phase of the interfering waves at the observing screen

- The spacing of fringes is set by the slit separation
- Phase = $2 \pi x d / a \lambda$
- $x_{max} = m\, a \lambda / d$, m = 0, 1, 2 , ...

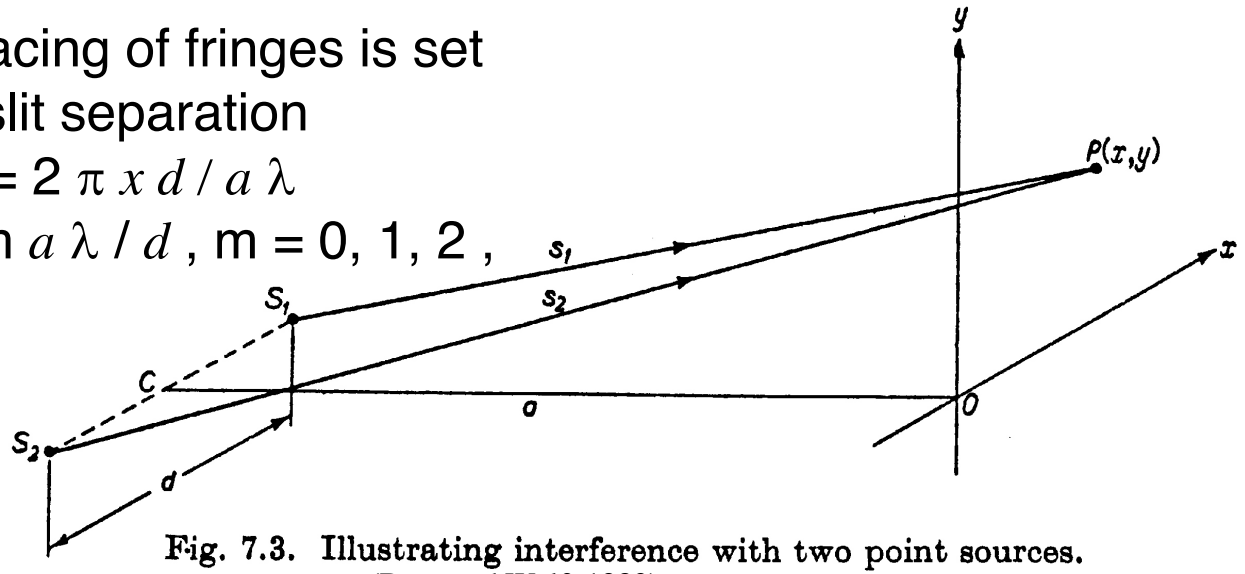

Fig. 7.3. Illustrating interference with two point sources.
(Born and Wolf, 1980)

Radar Interferometry

- Radar Interferometry is a simple extension of the Young's interferometry concept
- Radar has a coherent source much like a laser
- The two radar (SAR) antennas act as coherent point sources

- Because the wavelengths are so long, the signal can easily be digitized and processed coherently, measuring the phase information directly.
- When imaging a surface, the phase fronts from the two sources interfere.
- The surface topography slices the interference pattern.

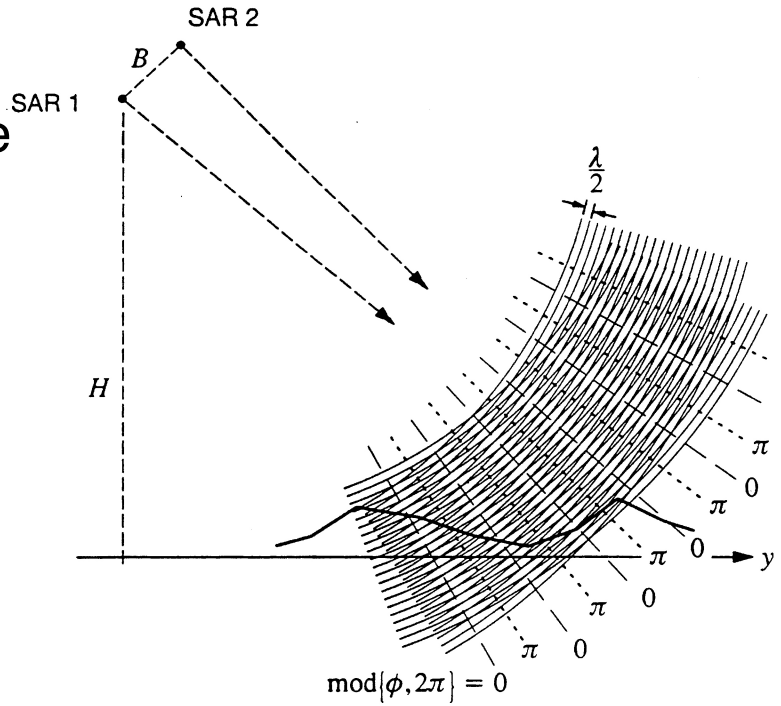

- The measured phase differences record the topographic information.

forming interferogram

$$C(\mathbf{x}) = A(\mathbf{x})e^{i\phi(\mathbf{x})} \tag{C1}$$

where $\mathbf{x} = (\rho, a)$ is the position vector consisting of range ρ and azimuth a. Their product is

$$C_2 C_1^* = A_1 A_2 e^{i(\phi_2 - \phi_1)} = R(\mathbf{x}) + iI(\mathbf{x}). \tag{C2}$$

The phase of the interferogram is extracted in the usual way.

$$(\phi_2 - \phi_1) = \tan^{-1}\left(\frac{I}{R}\right) \tag{C3}$$

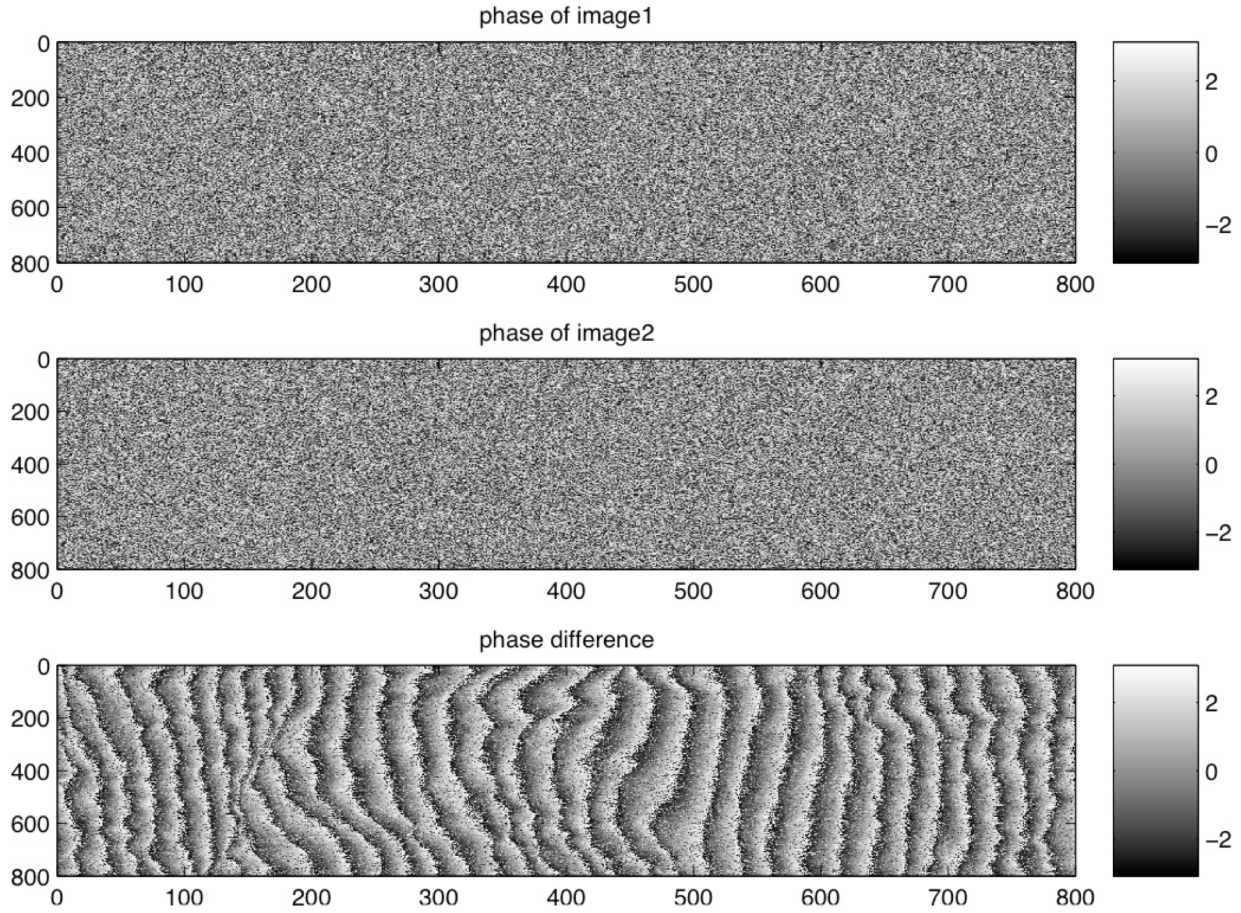

phase =

earth curvature (almost a plane, known) +
topographic phase (broad spectrum) +
surface deformation (broad spectrum, unknown) +
orbit error (almost a plane, largely known) +
ionosphere delay (a plane or 40-km wavelength waves) +
troposphere delay (power law, unknown) +
phase noise (white spectrum, unknown)

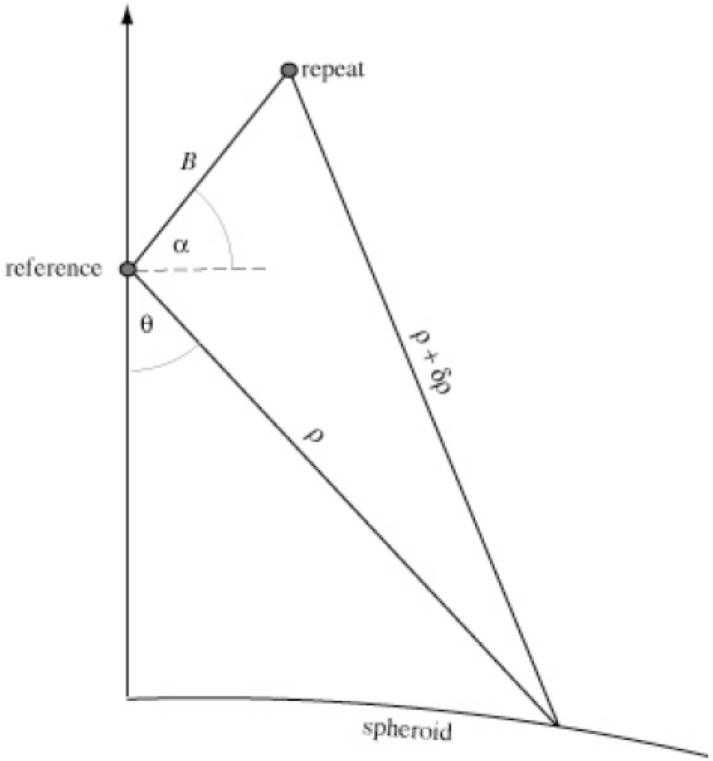

$$(\rho+\delta\rho)^2 = \rho^2 + B^2 - 2\rho B\sin(\theta-\alpha) \tag{C7}$$

Next we make two standard approximations that are useful for introducing interferometric concepts but are unnecessary and also lead to inaccurate results. First we assume $\delta\rho << \rho$ so we have

$$\delta\rho = \frac{B^2}{2\rho} - B\sin(\theta-\alpha)\,. \tag{C8}$$

Furthermore since $B << \rho$ the parallel ray approximation yields.

$$\phi = \frac{-4\pi}{\lambda} B\sin(\theta-\alpha) \tag{C9}$$

The phase difference depends on the parallel component of the baseline. The derivative of the phase with respect to range is

$$\frac{\partial\phi}{\partial\rho} = \frac{-4\pi}{\lambda} B\cos(\theta-\alpha)\frac{\partial\theta}{\partial\rho} \tag{C10}$$

Perpendicular baseline MATTERS!

$$B_{\parallel} = B\sin(\theta - \alpha)$$

$$B_{\perp} = B\cos(\theta - \alpha)$$

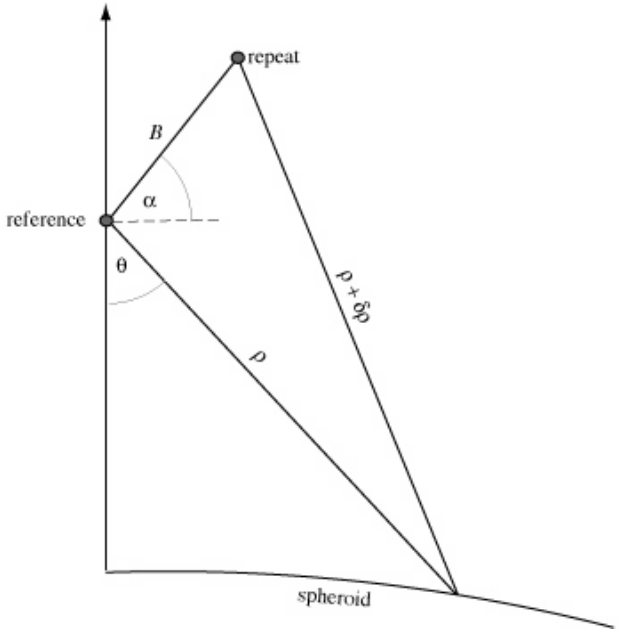

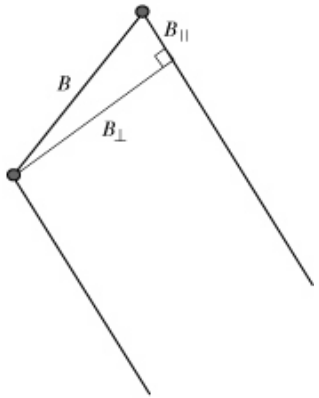

$$\frac{\partial\phi}{\partial\rho} = \frac{-4\pi B\cos(\theta - \alpha)}{\lambda\rho \quad \sin\theta}\left(\cos\theta - \frac{\rho}{b}\right)$$

phase due to curved earth

$$(\phi - \phi_e) \cong \frac{-4\pi r_e B\cos(\theta - \alpha)}{\lambda\rho b\sin\theta}(r - r_e)$$

phase due to topography

Phase from curved Earth

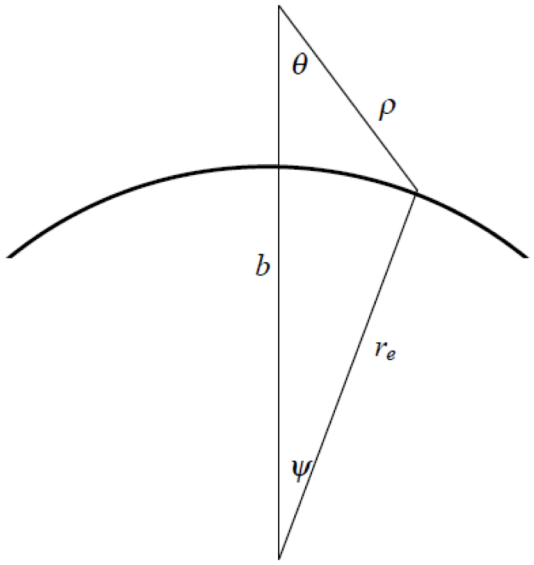

Figure C3 Triangle formed by the range ρ, radius of the earth r_e and spacecraft height b.

(from the center of the Earth!)

Using the Law of cosines one finds

$$\eta = \cos\theta = \frac{\left(b^2 + \rho^2 - r_e^2\right)}{2\rho b} \qquad \text{(C12)}$$

$$\frac{\partial\phi}{\partial\rho} = \frac{-4\pi B}{\lambda\rho}\frac{\cos(\theta-\alpha)}{\sin\theta}\left(\cos\theta - \frac{\rho}{b}\right)$$

fringe rate is higher for larger B…

total phase

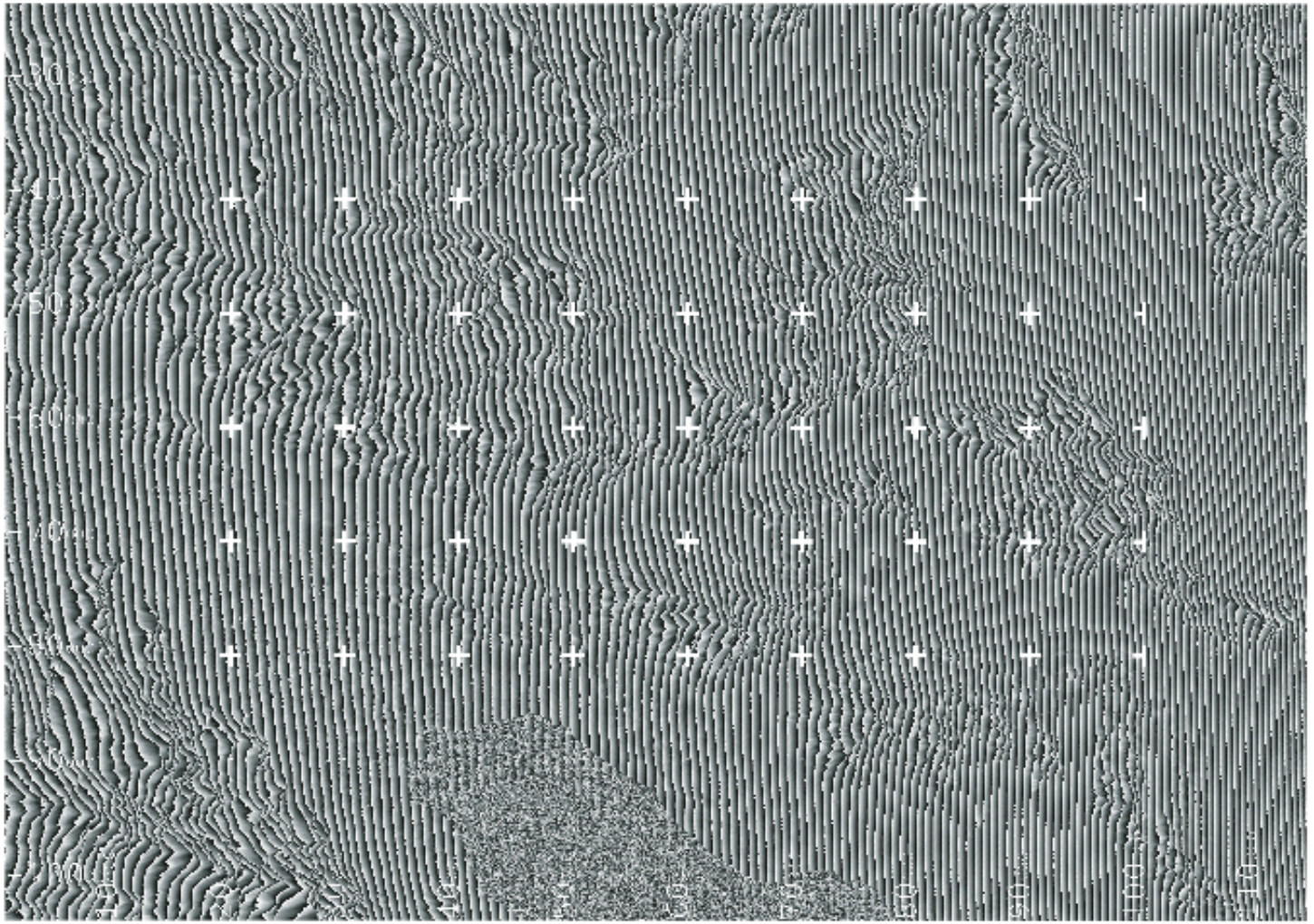

3) This is an interferogram made from ERS SAR data. One fringe represents 2 π phase change between the reference and repeat SAR acquisition. Count the fringes across the image and calculate the perpendicular baseline. You will need the look angle from the previous problem. The total change in slant range across the image is 50 km. Why does the fringe rate vary slightly across the image?

Critical Baseline

$$\frac{\partial\phi}{\partial\rho} = \frac{-4\pi B_{\perp}}{\lambda\rho}\frac{\cos\theta}{\sin\theta} < \frac{2\pi}{\Delta\rho}$$

$$B_c = \frac{\lambda\rho}{C\tau}\tan\theta \quad . \qquad \text{(C16)}$$

For the parameters of the ERS satellite the critical baseline is 1100 m (Tabel 1). For topographic recovery, a baseline of about 1/4 critical is optimal. Of course for change detection, a zero baseline is optimal but not usually available.

Table 1. Comparison of critical baseline

look angle	23°	34°	41°
ERS/ENVISAT 16 MHz	1.1 km	2.0	2.9
ALOS FBD 14 MHz	3.6	6.5	9.6
ALOS FBS 28 MHz	7.3	13.1	18.6

ERS/ENVISAT - altitude = 790 km, wavelength = 56 mm
ALOS - altitude = 700 km, wavelength = 236 mm
Shaded area is most common mode for interferometry.

Phase from topography

$$\frac{\partial \phi}{\partial r}(r_e) = \frac{-4\pi r_e}{\lambda \rho b} \frac{B\cos(\theta_e - \alpha)}{\sin\theta_e}$$

where θ_e is the look angle to the spheroid (C12).

into elevation as a function of range is

$$(r - r_e) = \frac{-\lambda \rho b}{4\pi r_e} \frac{\sin\theta_e}{B\cos(\theta_e - \alpha)} (\phi - \phi_e)$$

$$h_a = \frac{\lambda \rho \sin\theta_e}{2B_\perp} \qquad \text{(C21)}$$

For the case of ERS with a perpendicular baseline of 100 m, this altitude of ambiguity is about 90 m. For change detection, a higher number is better.

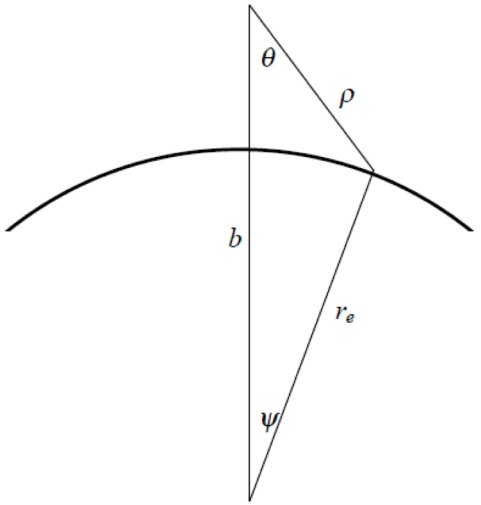

Figure C3 Triangle formed by the range ρ, radius of the earth r_e and spacecraft height b.

Using the Law of cosines one finds

$$\eta = \cos\theta = \frac{\left(b^2 + \rho^2 - r_e^2\right)}{2\rho b} \qquad \text{(C1}$$

phase minus spherical earth

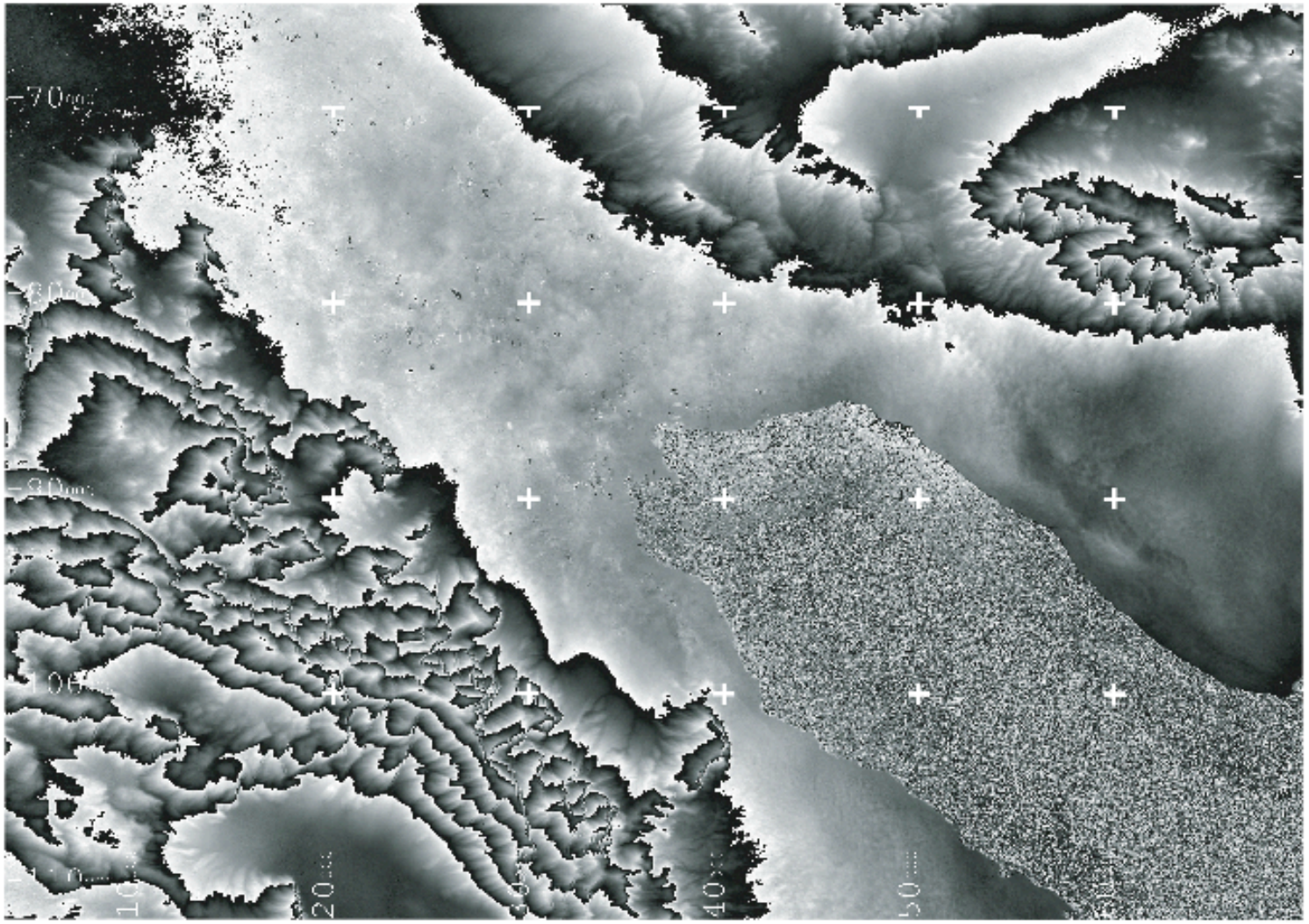

4) Interferogram with fringes due to geometry and Earth curvature removed. What are the cause(s) of the residual fringes? Why is the phase along the shoreline of the Salton Sea not exactly constant? (there are several possibilities).

deformation and topography

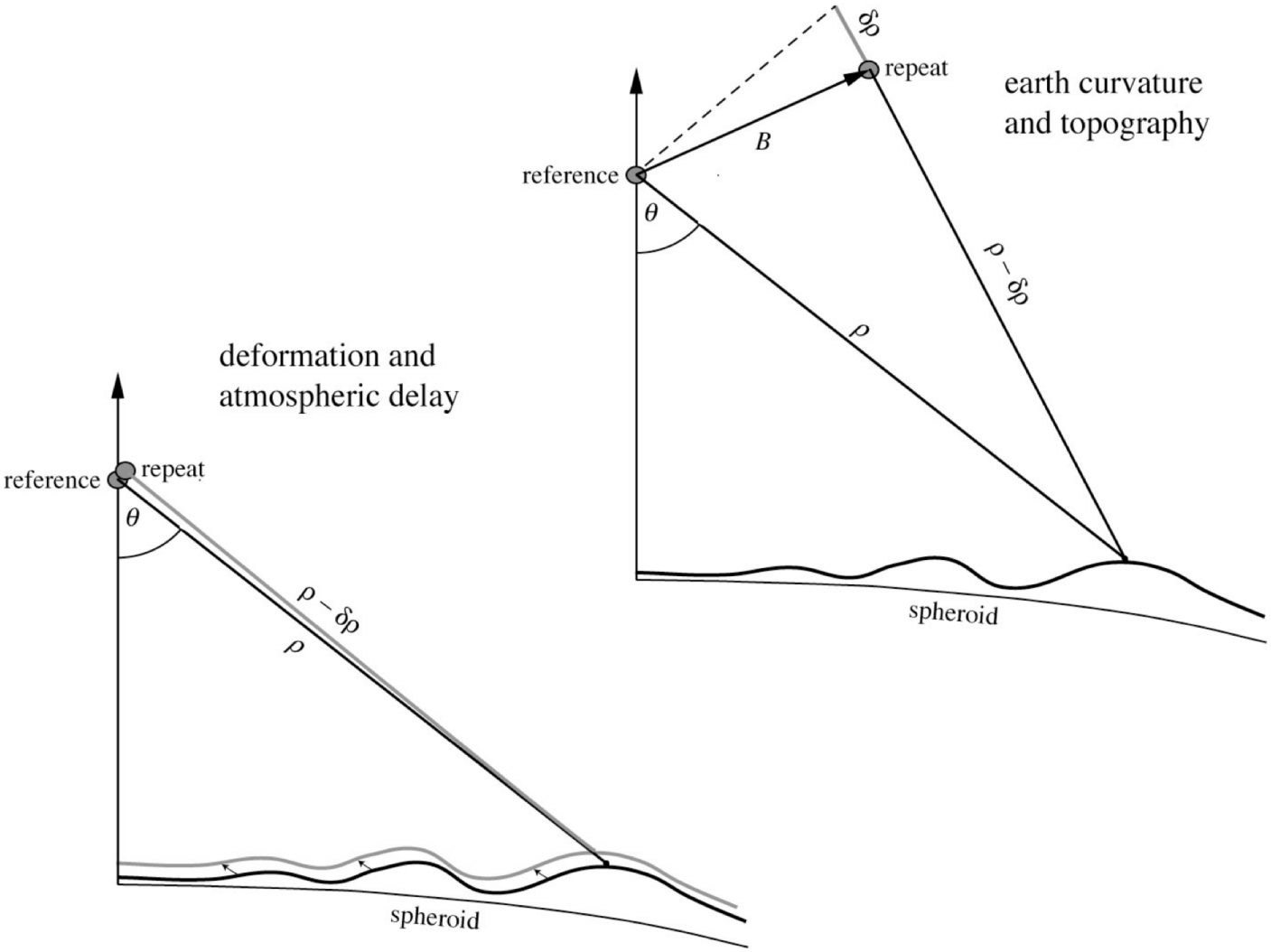

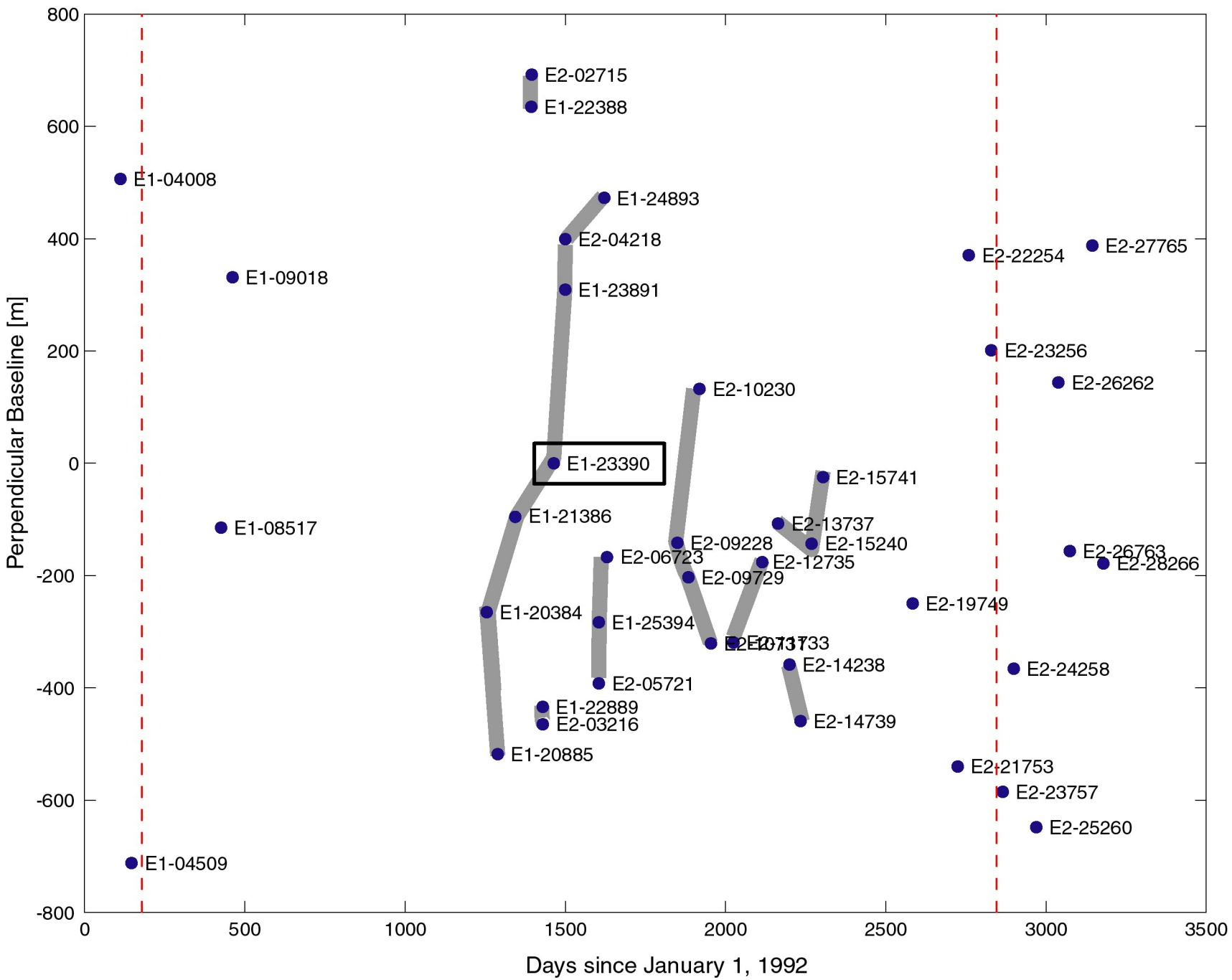
Topographic Pairs
Perpendicular Baseline [m]
Days since January 1, 1992
800
600
400
200
0
-200
-400
-600
-800
0
500
1000
1500
2000
2500
3000
3500
E2-02715
E1-22388
E1-04008
E1-24893
E2-04218
E2-22254
E2-27765
E1-09018
E1-23891
E2-23256
E2-26262
E2-10230
E1-23390
E2-15741
E1-21386
E2-13737
E1-08517
E2-09228
E2-15240
E2-26763
E2-06723
E2-12735
E2-28266
E2-09729
E2-19749
E1-20384
E1-25394
E2-14238
E2-24258
E2-05721
E1-22889
E2-03216
E2-14739
E1-20885
E2-21753
E2-23757
E2-25260
E1-04509

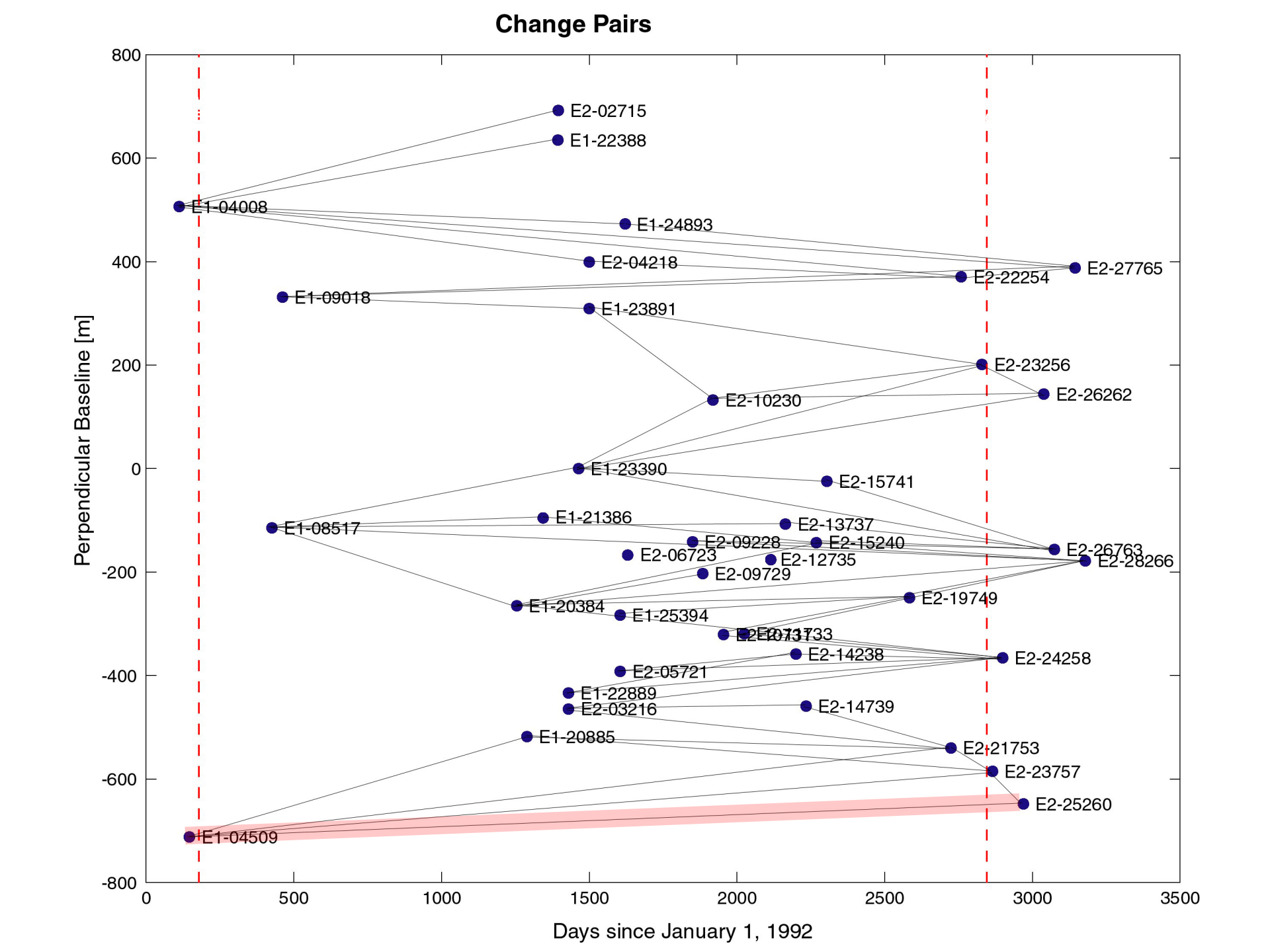
Change Pairs
Perpendicular Baseline [m]
Days since January 1, 1992
800
600
400
200
0
-200
-400
-600
-800
0
500
1000
1500
2000
2500
3000
3500
E2-02715
E1-22388
E1-04008
E1-24893
E2-04218
E2-27765
E2-22254
E1-09018
E1-23891
E2-23256
E2-26262
E2-10230
E1-23390
E2-15741
E1-08517
E1-21386
E2-13737
E2-09228
E2-15240
E2-26763
E2-06723
E2-12735
E2-28266
E2-09729
E1-20384
E2-19749
E1-25394
E2-14238
E2-24258
E2-05721
E1-22889
E2-03216
E2-14739
E1-20885
E2-21753
E2-23757
E2-25260
E1-04509

Interferometry Applications

- Mapping/Cartography

  Radar Interferometry from airborne platforms is routinely used to produce topographic maps as digital elevation models (DEMs).
  - 2-5 meter circular position accuracy
  - 5-10 m post spacing and resolution
  - 10 km by 80 km DEMs produced in 1 hr on mini-supercomputer

  Radar imagery is automatically geocoded, becoming easily combined with other (multispectral) data sets.

  Applications of topography enabled by interferometric rapid mapping
  - Land use management, classification, hazard assessment, intelligence, urban planning, short and long time scale geology, hydrology
- Deformation Mapping and Change Detection

  Repeat Pass Radar Interferometry from spaceborne platforms is routinely used to produce topographic *change* maps as digital displacement models (DDMs).
  - 0.3-1 centimeter relative displacement accuracy
  - 10-100 m post spacing and resolution
  - 100 km by 100 km DDMs produced rapidly once data is available

  Applications include
  - Earthquake and volcano monitoring and modeling, landslides and subsidence
  - Glacier and ice sheet dynamics
  - Deforestation, change detection, disaster monitoring =